Chemical Engineering Journal 155 (2009) 654–659

Contents lists available at ScienceDirect

Chemical Engineering Journal

journal homepage: www.elsevier.com/locate/cej

Separation of *p*-chloronitrobenzene and *o*-chloronitrobenzene by selective adsorption using Silicalite-1 zeolite

Zhaobing Guo[a,*], Shourong Zheng[b], zheng Zheng[b]

[a] School of Environmental Science & Engineering, Nanjing University of Information Science & Technology, Ningliu Rd 219, Nanjing 210044, PR China
[b] State Key Laboratory of Pollution Control and Resource Reuse, School of the Environment, Nanjing University, Nanjing 210093, PR China

ARTICLE INFO

Article history:
Received 27 April 2009
Received in revised form 24 July 2009
Accepted 24 August 2009

Keywords:
Chloronitrobenzene
Silicalite-1 zeolite
Adsorption
Separation

ABSTRACT

Silicalite-1 zeolite was used for selective adsorption and separation of *p*-chloronitrobenzene (*p*-CNB) and *o*-chloronitrobenzene (*o*-CNB). Maximum adsorption amounts of *p*-CNB in the zeolite are found to be approximately 4 molecules per unit cell (mol./u.c.), much higher than those of *o*-CNB. *p*-CNB molecules are considered to be located in zeolite intersections and channels. CNBs adsorption in Silicalite-1 zeolite follows pseudo-second-order kinetic model. Adsorption amounts and temperatures are the important parameters in affecting CNBs adsorption rate constants. Adsorption rate constants of *p*-CNB are higher than those of *o*-CNB in Silicalite-1 zeolite. *p*-CNB with a purity of 94.9% and *o*-CNB of 96.1% can be recovered with Silicalite-1 zeolite under an optimal separation condition investigated. Compared with Silicalite-1 zeolite, the presence of acid sites in zeolites is not only favorable for *p*-CNB selective adsorption from CNBs aqueous solution, but also improves the adsorption heat of *p*-CNB.

1. Introduction

Chloronitrobenzenes (CNBs) are important organic intermediates, extensively applied to production of dyes, pesticides, pharmaceuticals and rubber chemicals. CNBs are commonly prepared by nitrification of chlorobenzene (CB). A large amount of wastewater, containing high concentration of *p*- and *o*-CNB, incurs in the process of CB nitrification. Based on high toxicity and stability of *p*- and *o*-CNB [1], they are resistant to biodegradation. Some investigations have demonstrated that the detoxification of wastewater containing these recalcitrant chemicals can be only achieved using advanced oxidation processes (AOPs), such as photo-catalysis [2,3], Fenton oxidation [4] and ultrasonication [5,6]. It should be pointed out that decomposition of these chemicals using AOPs might result in a high treatment cost and resource waste. Therefore, there is a growing need to recover valuable chemicals from wastewater in the viewpoint of clean production [7].

Adsorption is considered as one of appropriate approaches to recover valuable chemicals from wastewater. However, a mixture will be obtained if non-selective sorbents such as resin and activated carbon are used because wastewater usually contains many kinds of compounds. High-purity chemicals can be obtained by the further crystallization or distillation if these chemicals have different physicochemical properties. Separation becomes very difficult if the recovered mixture consists of isomers compounds. Thus, it is highly desirable to directly recover these high-purity chemicals from wastewater by selective adsorption.

MFI-type zeolites are the most frequently studied zeolitic materials, which are the medium-pore aluminosilicates consisting of a three-dimensional interconnected channel system with 10-membered openings (0.51 nm × 0.55 nm and 0.53 nm × 0.56 nm) and intersections (1.0 nm) [8–10]. Due to similar dimensions of its channels to kinetic diameter of benzene molecule (0.58 nm), MFI type zeolites are frequently used as selective catalyst or adsorbent in aromatic compounds involved processes [11–13]. Adsorption and separation of aromatic compounds in MFI type zeolites depend not only on their shape selectivity effect, but also on the aluminum content (acid sites) in zeolite framework [14]. Silicalite-1 is an all-silica MFI zeolite, and HZSM-5 zeolite has an iso-structural framework, in which some of the Si atoms are substituted with Al. It possesses acidic properties because of the protons that provide electrical neutrality of the zeolite. We have studied the recovery of *p*-CNB using HZSM-5 zeolite (Si/Al = 43) and found that *p*-CNB could be effectively separated from *o*-CNB in aqueous solution [15]. To make clear the selective adsorption of *p*-CNB in different MFI type zeolites, in the present work, we made a further investigation on the adsorption and separation of *p*-CNB and *o*-CNB using Silicalite-1 zeolite. Furthermore, we explored the influence of the acid sites in zeolite framework on CNBs adsorption properties and heat of adsorption by comparing with the adsorption of CNBs in HZSM-5 zeolite.

* Corresponding author. Tel.: +86 25 82029166; fax: +86 25 58731090.
E-mail address: guozbnuist@163.com (Z. Guo).

1385-8947/$ – see front matter © 2009 Elsevier B.V. All rights reserved.
doi:10.1016/j.cej.2009.08.022

2. Materials and methods

2.1. Materials

Silicalite-1 zeolite was purchased from Kailida Power Industry CO. LTD. China with an average particle diameter of 5 μm, BET surface area of 279 m^2/g, chemical composition for unit cell of $Na_{0.17}Al_{0.17}Si_{95.83}O_{192}\cdot 16H_2O$ and the corresponding molar mass of 6052 g/mol. *p*-CNB (>99.5%) and *o*-CNB (>99.5%) were obtained from Shanghai Chemicals Factory. All chemicals are used without further purification.

2.2. Adsorption experiments

Adsorption isotherms of *p*- or *o*-CNB in Silicalite-1 zeolite at different temperatures were determined using batch adsorption experiments [11]. Zeolite particles with the mass varying from 30 to 800 mg were charged into flasks containing 50 mL 125 mg/L of *p*-CNB or 150 mg/L of *o*-CNB stock solution. Then, these flasks were sealed and transferred into an incubator (Jieruier, ZD-88), in which adsorption temperature was, respectively, controlled at 278, 300 or 323 K. Under continuous shaking, adsorption process remained 48 h in order to reach adsorption equilibrium. Zeolite particles were removed by fast filtration and equilibrium concentration of *p*- or *o*-CNB solutions was determined using a UV-Vis spectrometer (Helios Beta) with detecting wave-length of *p*-CNB at 285 nm and *o*-CNB at 270 nm.

2.3. Adsorption kinetics

Adsorption kinetics of *p*- and *o*-CNB in Silicalite-1 zeolite was investigated by determining the time-resolved uptakes. 20 mL of distilled water was mixed with a known amount of the zeolite sample in a 500 mL flask for 10 min. 380 mL 79 mg/L *p*-CNB or *o*-CNB solution was then introduced into the flask and the mixture was stirred (200 r/min) at 278 and 300 K, respectively. Samples were taken with 10 mL syringe tube at preset time intervals and zeolite particles were separated quickly from solution by using disposable filter. Similarly, at 300 K, 0.2 g Silicalite-1 zeolites were mixed with 400 mL 37.5, 75 and 105 mg/L *p*-CNB, and 0.6 g Silicalite-1 zeolites were mixed with 400 mL 37.5, 50 and 75 mg/L *o*-CNB to evaluate the effect of CNBs concentrations on adsorption kinetics. Residual concentration of *p*- or *o*-CNB in the solution was determined spectrophoto-metrically.

2.4. Selective adsorption

Selective adsorption of *p*-CNB from an artificial wastewater containing *p*- and *o*-CNB was carried out at 278 and 300 K using Silicalite-1 zeolite. In a 500 mL flask, 300 mg of zeolite sample was suspended in 20 mL distilled water. 380 mL solution containing 36.3 mg/L *p*-CNB and 19.6 mg/L *o*-CNB was then added into the flask under continuous stirring. The solution was sampled at different time intervals and residual concentrations of *p*- and *o*-CNB in the solution were determined using a high-pressure liquid chromatography (HPLC, Agilent-1100). Detecting wave-length was set at 270 nm and detector temperature at 301 K. Blank experiments of *p*- and/or *o*-CNB adsorption indicated that the evaporation of the solutes was negligible under our experimental conditions.

2.5. Desorption experiment

The desorption of *p*-CNB from the Silicalite-1 zeolite was conducted at 300 K using ethanol as the eluent. The desorption efficiency of *p*-CNB is defined as:

$$E = \frac{C_{pe}V_e}{mQ_{pz}} \quad (1)$$

E denotes the desorption efficiency (%); C_{pe} the concentration of *p*-CNB in the eluent (mg/L); V_e the volume of the eluent (L); m the mass of the used zeolite sample (g) and Q_{pz} the amount of *p*-CNB adsorbed in the zeolite before desorption (mg/g).

All the experiments in this study were conducted in duplicate; the averages were calculated to describe the adsorption of CNBs in Silicalite-1 zeolite.

3. Results and discussion

3.1. FT-IR analysis on the zeolites

Fourier transform infrared spectroscopy (FT-IR, NEXUS870, USA) analyses were performed in the two zeolites (Fig. 1). The absorbance peak at 3607 cm^{-1} is indicative of the stretching vibration peak of ·OH, the stronger absorbance peak at 3607 cm^{-1} in HZSM-5 zeolite shows the more ·OH and acid sites [16]. The zeolite acidities can also be described as their Si/Al ratios. Based on half-quantitative analyses, the Si/Al ratios in HZSM-5 and Silicalite-1 zeolites are approximately 43 and 1120, respectively. The lack of Al in Silicalite-1 zeolite indicates the markedly weak acidity in Silicalite-1 zeolite than that in HZSM-5 zeolite.

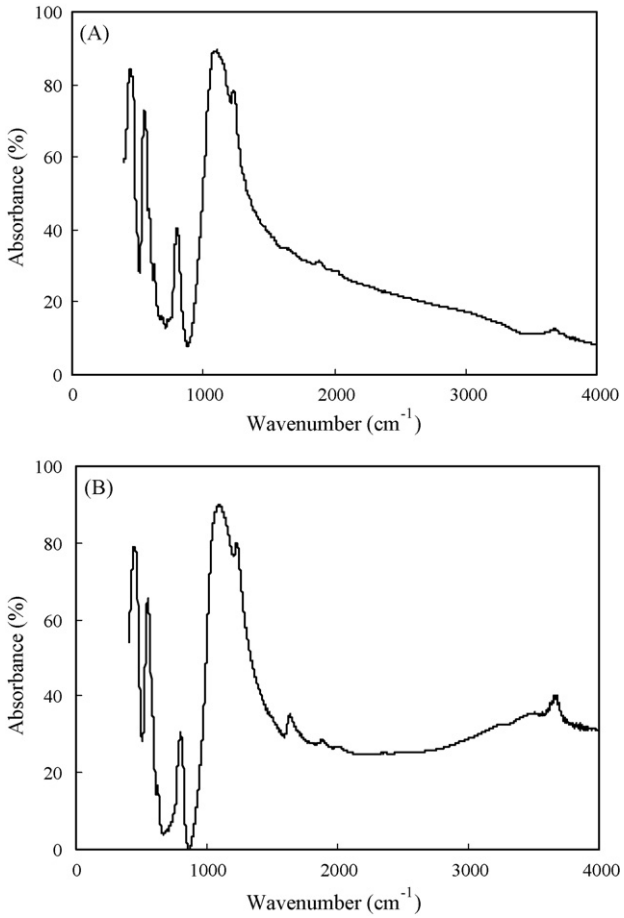

Fig. 1. FT-IR of Silicalite-1 (A) and HZSM-5 (B) zeolites.

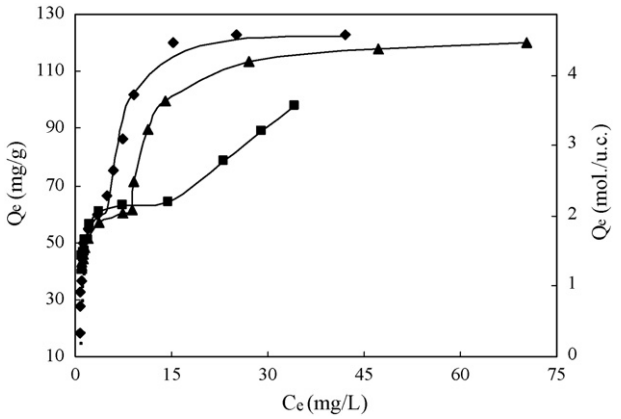

Fig. 2. Adsorption isotherms of *p*-CNB in Silicalite-1 zeolite at different temperatures. (♦) 278 K; (▲) 300 K; (■) 323 K; symbols: experimental data; full lines: fitting curves using Eq. (2).

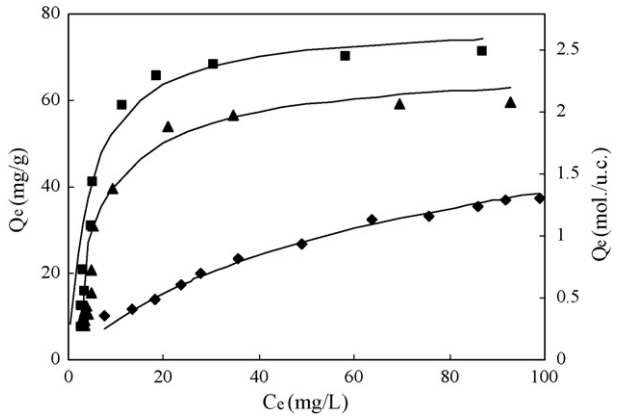

Fig. 3. Adsorption isotherms of *o*-CNB in Silicalite-1zeolite at different temperatures. (♦) 278 K; (▲) 300 K; (■) 323 K; symbols: experimental data; full lines: fitting curves using Eq. (3).

3.2. Adsorption isotherms

The dependences of adsorption amounts of *p*- and *o*-CNB in Silicalite-1 zeolite on equilibrium concentrations are described in Figs. 2 and 3. Adsorption isotherms of *p*-CNB in Silicalite-1 zeolite show clear steps at different adsorption temperatures and equilibrium adsorption amounts of *p*-CNB where the first step occur are found to be about 62 mg/g, corresponding to a molecular loading of about 2 mol./u.c. However, clear steps are not observed in *o*-CNB adsorption isotherms.

Adsorption isotherms of *p*-CNB in Silicalite-1 zeolite can be well described using a modified bimodal Langmuir adsorption model [17],

$$Q_e = \frac{Q_1 b_1 C_e}{1 + b_1 C_e} \qquad C_e \le C_s$$
$$Q_e = \frac{Q_1 b_1 C_e}{1 + b_1 C_e} + \frac{Q_2 b_2 (C_e - C_s)}{1 + b_2 (C_e - C_s)} \qquad C_e \ge C_s \tag{2}$$

Table 2
Parameters of *o*-CNB adsorption isotherms in Silicalite-1 zeolite.

T (K)	Q_0		b	n	R^2
	mg/g	mol./u.c.			
278	41.9	1.5	0.02	0.9	0.996
300	68.9	2.4	0.19	0.88	0.997
323	78.1	2.7	0.23	0.98	0.973

where Q_e is equilibrium adsorption amount (mg/g) at *p*-CNB equilibrium concentration C_e (mg/L); C_s is equilibrium concentration at which the first step ends (mg/L); Q_1 and Q_2 are maximum adsorption amounts of *p*-CNB in different parts of adsorption isotherms (mg/g); b_1 and b_2 are adsorption parameters.

In contrast, *o*-CNB adsorption in the zeolite follows typical Langmuir–Friendlich adsorption model [18],

$$Q_e = \frac{Q_0 b C_e^n}{1 + b C_e^n} \tag{3}$$

where Q_e is equilibrium adsorption amount (mg/g) at equilibrium concentration C_e (mg/L); Q_0 is maximum adsorption amount (mg/g); b and n are adsorption parameters.

Simulation results of adsorption isotherms are listed in Tables 1 and 2. Maximum adsorption amounts of *p*-CNB in Silicalite-1 zeolite are observed to be about 4.3 mol./u.c. at different adsorption temperatures. Adsorption of *p*-CNB in Silicalite-1 zeolite is considered to be a volume filling of the zeolite microporous adsorption space. The channels and the intersections are two different possible adsorption sites in Silicalite-1 zeolite. Klemm et al. [19] revealed that aromatic compounds were preferentially located the intersections due to higher potential energy of *p*-CNB adsorbed in the channels compared to that in the intersections of MFI type zeolites. Considering that there are 4 intersections per unit cell of MFI type zeolites, which is identical to maximum adsorption amounts of *p*-CNB in Silicalite-1 zeolite, we can conclude that *p*-CNB molecules were adsorbed in the intersections of the zeolite with their tails and heads pointing into the channels. The complete occupation of zeolite intersections and channels results in the same *p*-CNB maximum adsorption amounts in Silicalite-1 zeolite at different temperatures. This further demonstrates that *p*-CNB adsorption in Silicalite-1 zeolite is not as a surface coverage, but as a volume filling. Due to longer length of *p*-CNB molecule (1.07 nm) than the distance between vicinal intersections of the zeolite (1.0 nm), the tails and heads of *p*-CNB molecules in zeolite channels are inevitably overlapped. The molecular interactions between *p*-CNB absorbed in Silicalite-1 zeolite lead to clear steps in *p*-CNB adsorption isotherms.

b_1 and b_2 values are indicative of the interactions between *p*-CNB and zeolites, high b values are related to their strong interactions. The lower b_1 values in Silicalite-1 zeolite compared to those in HZSM-5 zeolite suggest different adsorption behaviors and interactions between *p*-CNB and zeolite framework at the molecule loading lower than 2 mol./u.c. [15]. As the same MFI-type zeolite, the framework structures of Silicalite-1 and HZSM-5 zeolites are identical except the presence of more acid sites in HZSM-5 zeolite. The Si/Al ratio of HZSM-5 zeolite was measured to be 43, indicating that there are about 2 intersections with acid OH group per unit cell of HZSM-5 zeolite. Compared to those in Silicalite-1 zeolite, the

Table 1
Parameters of *p*-CNB adsorption isotherms in Silicalite-1 zeolite.

T (K)	Q_1		Q_2		$Q_1 + Q_2$		b_1	b_2	C_s (mg/L)	R^2
	mg/g	mol./u.c.	mg/g	mol./u.c.	mg/g	mol./u.c.				
278	65.5	2.3	61.5	2.1	127.0	4.4	2.1	0.41	5.2	0.987
300	64.9	2.3	58.2	2.0	123.1	4.3	1.9	0.19	8.5	0.992
323	65.8	2.3	57.8	2.0	123.6	4.3	1.1	0.08	15	0.973

higher b_1 values and identical b_2 values in HZSM-5 zeolite shows that *p*- CNB molecules are preferentially located in HZSM-5 intersections with acid sites at molecule loading lower than 2 mol./u.c.

It is also noteworthy that maximum adsorption amounts of *o*-CNB are lower than those of *p*-CNB in Silicalite-1 zeolite. This is related to their kinetic diameters of *p*-CNB and *o*-CNB. *p*-CNB molecules can easily diffuse into the pores of Silicalite-1 zeolite and occupy zeolite intersections and channels due to its similar kinetic diameter (0.58 nm) to the dimensions of zeolite channels. However, *o*-CNB molecules are hindered from penetrating into the pores of Silicalite-1 zeolite for the large kinetic diameter of 0.75 nm.

Meanwhile, we find that maximum adsorption amounts of *o*-CNB in Silicalite-1 zeolite were higher compared to those in HZSM-5 zeolite. It is ascribed to the acid sites locating in pore mouth of HZSM-5 zeolite, which can absorb H_2O molecules and narrow of pore openings of the zeolite [20]. Besides, the flexibility of the MFI structure is reduced when aluminum is introduced in zeolite. The almost aluminum-free in Silicalite-1 zeolite is favorable for broadening pore openings and increasing its hydrophobicity, thereby driving *o*-CNB into the zeolite pore [21].

On the basis of *p*-CNB adsorption isotherms, we obtained the adsorption heats of *p*-CNB in Silicalite-1 zeolite at different molecular loadings (Fig. 4) according to Clausius–Clapeyron equation [22],

$$\Delta H_{ads} = \frac{d\ln(C_e)}{d(1/T)_{Q=const}} \quad (4)$$

where ΔH_{ads} is adsorption heat (kJ/mol); C_e is equilibrium concentration of *p*-CNB (mg/L) at constant adsorption amount Q (mg/g) and T (K) is adsorption temperature.

As Fig. 4 indicates, *p*-CNB heats adsorption in Silicalite-1 zeolite are lower than 25 kJ/mol. Adsorption heats at *p*-CNB loadings lower than 2 mol./u.c. are found to be much lower than those at molecular loadings between 2 and 4 mol./u.c. This is attributed to molecular interactions of absorbed *p*-CNB and the change in molecular loading on adsorption sites with different potential energies. At *p*-CNB loadings higher than 4 mol./u.c. decreased adsorption heats are observed suggesting that some *p*-CNB molecules are absorbed in the zeolite pore opening.

At *p*-CNB loading lower than 2 mol./u.c. adsorption heats in Silicalite-1 and HZSM-5 zeolites are approximately 10 and 15 kJ/mol [15], respectively. Higher adsorption heats in HZSM-5 zeolite result from hydrogen bonding interaction of *p*-CNB molecules with SiAlOH groups in the intersections of HZSM-5 zeolite [23]. At *p*-CNB loadings higher than 2 mol./u.c. higher heat in HZSM-5 zeolite (31 kJ/mol) is also observed compared to that in Silicalite-1 zeolite (22 kJ/mol).

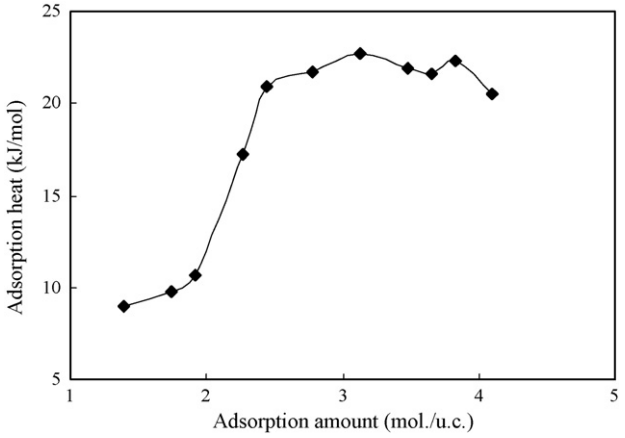

Fig. 4. Dependence of adsorption heats on *p*-CNB molecular loading in Silicalite-1 zeolite.

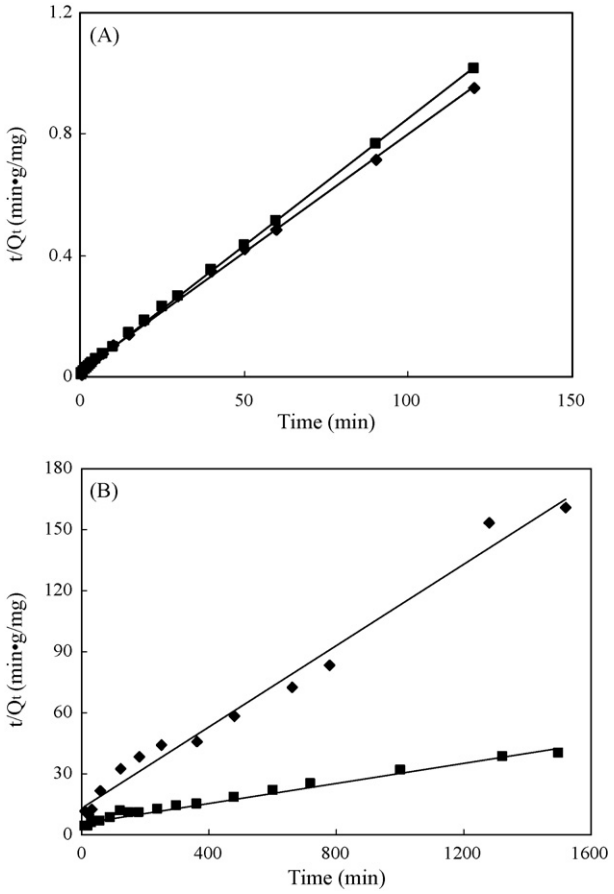

Fig. 5. Simulation of *p*-CNB (A) and *o*-CNB (B) adsorption in Silicalite-1 zeolite at different temperatures. (♦) 278 K; (■) 300 K; symbols: experimental data; lines: fitting lines using Eq. (5).

3.3. Adsorption kinetics of CNBs in the zeolite

Adsorption kinetics of sorbate molecules in porous materials can be determined using time-resolved uptake. In this contribution, time-resolved uptakes of *p*- and *o*-CNB in Silicalite-1 zeolite at different temperatures and initial concentrations are carried out respectively.

Pseudo-second-order kinetics is based on adsorption capacity, which usually gives a good description of the whole adsorption process. Therefore, the adsorption of *p*- and *o*-CNB in Silicalite-1 zeolite was simulated using pseudo-second-order kinetic model in this study. Pseudo-second-order kinetic model can be expressed as the equation [24],

$$\frac{t}{Q_t} = \frac{1}{kQ_e^2} + \frac{1}{Q_e}t \quad (5)$$

where Q_e is equilibrium adsorption amount (mg/g), Q_t (mg/g) is adsorption amount at time t (min), and k is pseudo-second-order rate constant (g/mg/min).

The plots of t/Q_t versus t are compiled in Figs. 5 and 6, and the corresponding simulation parameters are listed in Tables 3 and 4. The good linear plots of t/Q_t versus t with the correlation coefficients (R^2) higher than 0.98 suggest that *p*- and *o*-CNB adsorption in Silicalite-1 zeolite predominantly follows pseudo-second-order kinetic model.

It is observed from Table 3 that adsorption rate constant of *p*-CNB in Silicalite-1 zeolite (7.4×10^{-3} g/mg/min) at 300 K is higher compared to that (3.6×10^{-3} g/mg/min) in 278 K under similar equilibrium adsorption amounts. High temperature can

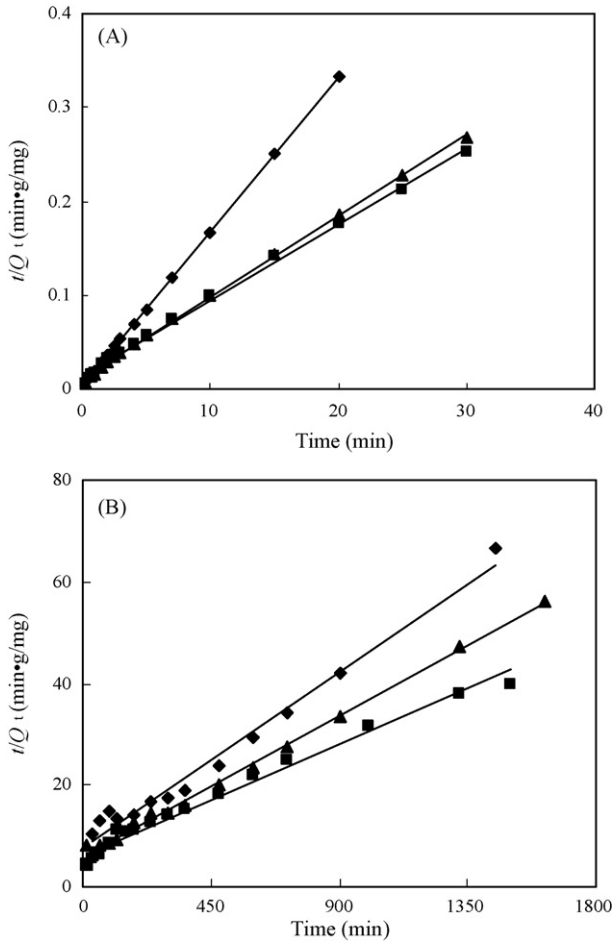

Fig. 6. Simulation of *p*-CNB (A) and *o*-CNB (B) adsorption in Silicalite-1 zeolite at different concentrations. For *p*-CNB, (♦) 37.5 mg/L; (▲) 75 mg/L; (■) 105 mg/L; for *o*-CNB, (♦) 37.5 mg/L; (▲) 50 mg/L; (■) 75 mg/L; symbols: experimental data; lines: fitting lines using Eq. (5).

increase molecular energy and favor *p*-CNB penetrations into zeolite pores. However, we also note that adsorption rate constant of *o*-CNB (1.0×10^{-4} g/mg/min) at 300 K is only one-tenth to that (9.9×10^{-4} g/mg/min) at 278 K under similar equilibrium adsorption concentrations. It should be pointed out that the corresponding equilibrium adsorption amounts of *o*-CNB in Silicalite-1 zeolite at 278 and 300 K are 14.5 and 43.5 mg/g, respectively. This indicates that adsorption amount of CNBs in the zeolite is a very important parameter in controlling the rate constants. This conclusion was further confirmed by the effect of CNBs initial concentrations on their rate constants in this study (Table 4). For *o*-CNB, the rate constants decrease with the increasing equilibrium adsorption amounts. And for *p*-CNB, the rate constant at the molecular loading of 2 mol./u.c. is beyond 10 times higher compared to that at the molecular loading of 4 mol./u.c. The higher adsorption amounts of *p*- and *o*-CNB in Silicalite-1 zeolite mean the less empty adsorption sites and the stronger molecular interactions, which are unfavorable for *p*- and *o*-CNB diffusion into zeolite channels.

In addition, the adsorption of *p*-CNB molecules is observed to be much faster than that of *o*-CNB molecules in Silicalite-1 zeolite. For the configurational diffusion, a minor difference between kinetic diameters of sorbate molecules can result in a marked difference in their adsorption rate constants [25]. The kinetic diameters of *p*- and *o*-CNB molecules are estimated to be 0.58 and 0.75 nm, respectively, which leads to markedly fast adsorption of *p*-CNB in the pores of Silicalite-1 zeolite.

3.4. Selective adsorption

The selection adsorption efficiency of *p*-CNB from *p*- and *o*-CNB solution is usually described by separation factor of *p*-CNB, which is defined as [26]:

$$\alpha_{po} = \frac{\chi_p^z \chi_o^l}{\chi_p^l \chi_o^z} \quad (6)$$

where α_{po} denotes the separation factor of *p*-CNB; χ_p^l and χ_p^z the mole fractions of *p*-CNB in the aqueous phase and adsorbed in the zeolite; χ_o^l and χ_o^z the mole fractions of *o*-CNB in the liquid phase and in the zeolite.

The separation factors of *p*-CNB at 278 and 300 K are compared in Fig. 7. The separation factors are found to be 178 and 87 after adsorption equilibrium at 278 and 300 K, respectively, suggesting that low temperature is favorable for *p*-CNB separation efficiency.

For adsorption of CNBs mixture in Silicalite-1 zeolite, Adsorption amounts of *p*-CNB and *o*-CNB were measured to be 44.8 and 9.5 mg/g at *p*-CNB equilibrium concentration of 0.9 mg/L and *o*-CNB of 16.5 mg/L at 300 K. This shows that *p*-CNB with a purity of 82.5% is selectively adsorbed in Silicalite-1 zeolite and *o*-CNB with a purity of 94.8% is residual in the solution. Similarly, 86.7% *p*-CNB and 95.9% *o*-CNB can be achieved by the separation of Silicalite-1 zeolite at 278 K. It is noteworthy from Fig. 7 that the largest separation factors occur after 20–30 min adsorption when *p*-CNB reaches adsorption equilibrium in Silicalite-1 zeolite. The purities of recov-

Table 3
Simulation parameters of *p*- and *o*-CNB adsorption in Silicalite-1 zeolite at different temperatures using pseudo-second-order kinetic model.

Sample	T (K)	C_e (mg/L)	k (g/mg/min)	Q_e(exp) (mg/g)	Q_e(cal) (mg/g)	R^2
p-CNB	278	9.3	3.6×10^{-3}	107.7	115.2	0.999
	300	17.0	7.4×10^{-3}	116.0	114.9	0.999
o-CNB	278	10.2	9.9×10^{-4}	14.5	10.1	0.984
	300	9.8	1.0×10^{-4}	43.5	40.8	0.983

Table 4
Simulation parameters of *p*- and *o*-CNB adsorption in Silicalite-1 zeolite at different initial concentrations using pseudo-second-order kinetic model.

Sample	C_0 (mg/L)	C_e (mg/L)	k (g/mg/min)	Q_e(exp) (mg/g)	Q_e(cal) (mg/g)	R^2
p-CNB	37.5	7.3	8.3×10^{-2}	60.4	60.6	1
	75.0	17.0	7.4×10^{-3}	116.0	114.9	0.999
	105	45.4	5.0×10^{-3}	119.2	123.5	0.996
o-CNB	37.5	4.7	1.8×10^{-4}	21.9	26.2	0.981
	50.0	5.2	1.6×10^{-4}	29.9	32.7	0.997
	75.0	9.8	1.0×10^{-4}	43.5	40.8	0.983

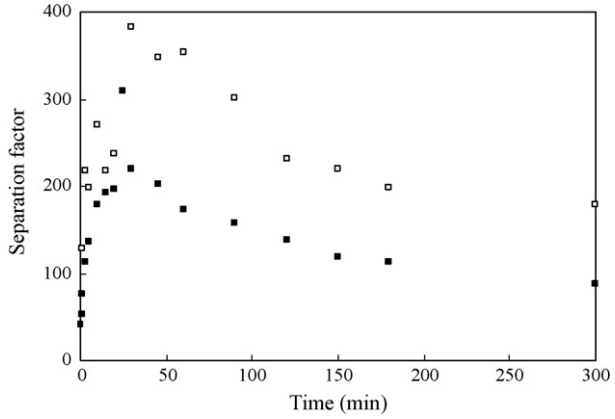

Fig. 7. Time-resolved separation factors of *p*-CNB at different adsorption temperatures in Silicalite-1 zeolite. Open symbols denote the separation factors at 278 K and filled symbols at 300 K.

ered *p*-CNB under this optimal condition, respectively, increase up to 94.9% and 92.0% at 278 and 300 K, and the corresponding purities of recovered *o*-CNB are 96.1% and 96.8%. Compared with HZSM-5 zeolite, a slight decrease in the recovery purities of *p*-CNB and *o*-CNB using Silicalite-1 zeolite is mainly attributed to the presence of acid sites in pore mouth of HZSM-5 zeolite, which can suppress *o*-CNB adsorption into zeolite channels.

Desorption efficiency of *p*-CNB from Silicalite-1 zeolite using ethanol is higher than 99% at 300 K, indicating that absorbed *p*-CNB in Silicalite-1 zeolite can be effectively recovered and obtain high-purity *p*-CNB from aqueous solution.

4. Conclusions

Selective adsorption and separation of *p*-CNB and *o*-CNB using Silicalite-1 zeolite was investigated. *p*-CNB molecules occupy channel intersections of the zeolite with their tails and heads pointing into the channels. *p*-CNB is preferentially absorbed in the zeolite intersections with acid sites. The adsorption temperature and adsorption amounts are the key factors in controlling adsorption rate constants of CNBs in Silicalite-1 zeolite. Equilibrium adsorption amounts and adsorption rate constants of *p*-CNB are higher than those of *o*-CNB in Silicalite-1 zeolite. The marked differences in adsorption amounts and adsorption rate constants between *p*-CNB and *o*-CNB lead to high separation efficiency of the zeolite. Under the optimal adsorption conditions, 94.9% *p*-CNB and 96.1% *o*-CNB are recovered using Silicalite-1 zeolite. The presence of acid sites in zeolites has little influence on *p*-CNB adsorption, but hinders *o*-CNB adsorption, which may increase their separation efficiency from aqueous solution.

Acknowledgements

We gratefully acknowledge financial supports from Natural Science Foundation of Jiangsu Province (BK2009414), State Key Laboratory of Pollution Control and Resource Reuse (PCRRF07010), Jiangsu Provincial Key Laboratory of Coastal Wetland Bioresources and Environmental Protection (JLCBE07004) and project on Natural Science Foundation Research of Jiangsu Colleges (No. 07KJD610135).

References

[1] S.K. Hong, D.K. Anestis, J.G. Ball, In vitro nephrotoxicity induced by chloronitrobenzenes in renal cortical slices from Fischer 344 rats, Toxicol. Lett. 129 (2002) 133–141.
[2] J.M. Herrmann, Heterogeneous photocatalysis: fundamentals and applications to removal of various types of aqueous pollutants, Catal. Today 53 (1999) 115–129.
[3] K.O. Awitor, S. Rafqah, G. Geranton, Y. Sibaud, R.S.P. Bokalawela, J.D. Jemigen, M.B. Johnson, Photo-catalysis using titanium dioxide nanotube layers, J. Photochem. Photobiol. A: Chem. 199 (2008) 250–254.
[4] J.J. Pignatello, D. Liu, P. Huston, Evidence for additional oxidant in the photoassisted Fenton reaction, Environ. Sci. Technol. 33 (1999) 1832–1839.
[5] Z.B. Guo, R. Feng, J.H. Li, Z. Zheng, Y.F. Zheng, Degradation of 2,4-dinitrophenol by combining sonolysis and different additives, J. Hazard. Mater. 158 (2008) 164–169.
[6] Z.B. Guo, R. Feng, Ultrasonic irradiation-induced degradation of low-concentration bisphenol A in aqueous solution, J. Hazard. Mater. 163 (2009) 855–860.
[7] Z.Y. Xu, Q.X. Zhang, H.P. Fang, Applications of porous resin sorbents in industrial wastewater treatment and resource recovery, Crit. Rev. Environ. Sci. Technol. 33 (2003) 1–27.
[8] J. Weitcamp, Zeolites and catalysis, Solid State Ionics 131 (2000) 175–188.
[9] M. Yu, J.C. Wyss, R.D. Noble, J.L. Falconer, 2,2-Dimethylbutane adsorption and diffusion in MFI zeolite, Micropor. Mesopor. Mater. 111 (2008) 24–31.
[10] C. Chmelik, L. Heinke, J. Karger, W. Schmidt, D.B. Shah, J.M. Van Baten, R. Krishna, Inflection in the loading dependence of the Maxwell–Stefan diffusivity of isobutane in MFI zeolite, Chem. Phys. Lett. 459 (2009) 141–145.
[11] Z.B. Guo, S.R. Zheng, Z. Zheng, F. Jiang, L.Q. Chen, Y.J. Wang, Study on adsorption and separation of chloronitrobenzene mixtures in aqueous phase using MFI-type zeolite, Acta Scientiae Circumstantiae 25 (2005) 773–778 (in Chinese).
[12] Y.P. Zeng, S.G. Ju, Adsorption of thiophene and benzene in sodium-exchanged MFI- and MOR-type zeolites: a molecular simulation study, Sep. Purif. Technol. 67 (2009) 71–78.
[13] A.M. Avila, U. Segran, Separation of ternary hydrocarbon mixtures on Y zeolite membranes, Chem. Eng. J. 146 (2009) 338–344.
[14] A.F.P. Ferreira, M.C. Mittelmeijer-Hazeleger, A. Bliek, J.A. Moulijn, Influence of Si/Al ratio on hexane isomers adsorption equilibria, Micropor. Mesopor. Mater. 111 (2008) 171–177.
[15] Z.B. Guo, S.R. Zheng, Z. Zheng, F. Jiang, W.Y. Hu, L.N. Ni, Selective adsorption of p-chloronitrobenzene from aqueous mixture of p-chloronitrobenzene and o-chloronitrobenzene using HZSM-5 zeolite, Water Res. 39 (2005) 1174–1182.
[16] K. Suzuki, Y. Aoyagi, N. Katada, M. Choi, R. Ryoo, M. Niwa, Aciditi and catalytiv activity of mesoporous ZSM-5 in comparison with zeolite ZSM-5, A-MCM-41 and silica–alumina, Catal. Today 132 (2008) 38–45.
[17] W. Zhu, F. Kapteijn, B. Van Der Linden, J.A. Moulijn, Equilibrium adsorption of linear and branched C-6 alkanes on silicalite-1 studied by the tapered element oscillating microbalance, Phys. Chem. Chem. Phys. 3 (2001) 1755–1761.
[18] C.W. Cheung, J.F. Porter, G. Mckay, Sorption kinetic analysis for the removal of cadmium ions from effluents using bone char, Water Res. 35 (2001) 605–612.
[19] E. Klemm, J.G. Wang, G. Emig, A comparative study of the sorption of benzene and phenol in silicalite, HAlZSM-5 and NaAlZSM-5 by computer simulation, Micropor. Mesopor. Mater. 26 (1998) 11–21.
[20] H. Jobic, A. Tuel, M. Krossner, J. Sauer, Water in interaction with acid sites in H-ZSM-5 zeolite does not form hydroxonium ions. A comparison between neutron scattering results and abinitio calculations, J. Phys. Chem. 100 (1996) 19545–19553.
[21] J. Lu, F. Xu, D.J. Wang, J. Huang, W.M. Cai, The application of silicalite-1/fly ash cenosphere zeolite composite for the adsorption of methyl tert-butyl ether, J. Hazard. Mater. 165 (2009) 120–125.
[22] J. Farrell, C. Manspeaker, J. Luo, Understanding competitive adsorption of water and trichloroethylene in a high-silica Y zeolite, Micropor. Mesopor. Mater. 59 (2003) 205–214.
[23] F. Eder, M. Stockenhuber, J.A. Lercher, Bronsted acid site and pore controlled siting of alkane sorption in acidic molecular sieves, J. Phys. Chem. B 101 (1997) 5414–5419.
[24] J.S. Allen, B. Koumanova, Z. Kircheva, S. Nenkova, Adsorption of 2-nitrophenol by technical hydrolysis lignin: kinetics, mass transfer, and equilibrium studies, Ind. Eng. Chem. Res. 44 (2005) 2281–2287.
[25] C.N. Satterfield, Heterogeneous Catalysis in Industrial Practice, 2nd ed., McGraw-Hill, New York, 1991.
[26] G. Guo, Y. Long, Static equilibrium studies on separation of dichlorobenzene isomers on binder-free hydrophobic adsorbent of MFI type zeolite, Sep. Purif. Technol. 24 (2001) 507–518.